IAI Journals.ASM.org

RALP1 Is a Rhoptry Neck Erythrocyte-Binding Protein of *Plasmodium falciparum* Merozoites and a Potential Blood-Stage Vaccine Candidate Antigen

Daisuke Ito,[a] Tomoyuki Hasegawa,[a] Kazutoyo Miura,[b] Tsutomu Yamasaki,[a]* Thangavelu U. Arumugam,[a] Amporn Thongkukiatkul,[c] Satoru Takeo,[a]* Eizo Takashima,[a] Jetsumon Sattabongkot,[d] Eun-Taek Han,[e] Carole A. Long,[b] Motomi Torii,[f] Takafumi Tsuboi[a,g]

Division of Malaria Research, Proteo-Science Center,[a] and Venture Business Laboratory,[g] Ehime University, Matsuyama, Ehime, Japan; Laboratory of Malaria and Vector Research, National Institute of Allergy and Infectious Diseases, National Institutes of Health, Rockville, Maryland, USA[b]; Department of Biology, Faculty of Science, Burapha University, Chonburi, Thailand[c]; Mahidol Vivax Research Unit, Faculty of Tropical Medicine, Mahidol University, Bangkok, Thailand[d]; Department of Medical Environmental Biology and Tropical Medicine, School of Medicine, Kangwon National University, Chuncheon, Gangwon-do, Republic of Korea[e]; Division of Molecular Parasitology, Proteo-Science Center, Ehime University, Shitsukawa, Toon, Ehime, Japan[f]

Erythrocyte invasion by merozoites is an obligatory stage of *Plasmodium* infection and is essential to disease progression. Proteins in the apical organelles of merozoites mediate the invasion of erythrocytes and are potential malaria vaccine candidates. Rhoptry-associated, leucine zipper-like protein 1 (RALP1) of *Plasmodium falciparum* was previously found to be specifically expressed in schizont stages and localized to the rhoptries of merozoites by immunofluorescence assay (IFA). Also, RALP1 has been refractory to gene knockout attempts, suggesting that it is essential for blood-stage parasite survival. These characteristics suggest that RALP1 can be a potential blood-stage vaccine candidate antigen, and here we assessed its potential in this regard. Antibodies were raised against recombinant RALP1 proteins synthesized by using the wheat germ cell-free system. Immunoelectron microscopy demonstrated for the first time that RALP1 is a rhoptry neck protein of merozoites. Moreover, our IFA data showed that RALP1 translocates from the rhoptry neck to the moving junction during merozoite invasion. Growth and invasion inhibition assays revealed that anti-RALP1 antibodies inhibit the invasion of erythrocytes by merozoites. The findings that RALP1 possesses an erythrocyte-binding epitope in the C-terminal region and that anti-RALP1 antibodies disrupt tight-junction formation, are evidence that RALP1 plays an important role during merozoite invasion of erythrocytes. In addition, human sera collected from areas in Thailand and Mali where malaria is endemic recognized this protein. Overall, our findings indicate that RALP1 is a rhoptry neck erythrocyte-binding protein and that it qualifies as a potential blood-stage vaccine candidate.

Plasmodium falciparum is the most virulent malaria parasite of the four species infecting humans, affecting about 216 million individuals and killing about 0.7 million individuals in 2010 worldwide (1). Since the latter half of the 1950s, the appearance of malaria parasites with resistance to antimalarial drugs and of mosquito vectors with resistance to insecticides has highlighted the importance of malaria vaccine development. Although a number of vaccine candidates have been developed and tested in preclinical and clinical trials, only limited clinical success has been achieved with vaccines to date (2, 3). Therefore, discovery of novel vaccine candidates is currently an important step because of the renewed focus on control, local elimination, and eventual global eradication efforts (4).

The symptoms of malaria are caused by blood-stage cyclic infection and subsequent rupture of the host's erythrocytes by obligate asexual intracellular malaria parasites. Erythrocyte invasion by the merozoite, the invasive form of the blood-stage parasite exposed to human immunity, is mediated by a complex set of interactions between different parasite ligands and erythrocyte receptors (5–7). The ligands used by the merozoite during invasion are either expressed on the surface of the merozoite or discharged from specialized apical organelles (rhoptries, micronemes, and dense granules) (5–7). Among the apical organelles, rhoptries are the most prominent large secretory organelles present in pairs at the apical tip of the merozoite and their contents are thought to be important throughout the invasion processes, such as initial host cell sensing, tight-junction formation, and establishment of the parasitophorous vacuole (PV). After attachment of merozoites to erythrocytes, rhoptry proteins mediate direct high-affinity merozoite-erythrocyte interactions with micronemal proteins (7) that ultimately lead to tight-junction formation and irreversible commitment of the merozoite to invasion. The tight junction is characterized by an electron-dense thickening between the erythrocyte membrane and the merozoite, and its molecular makeup is not yet fully understood, although it is known to include a number of rhoptry neck proteins (RONs), as well as the micronemal protein AMA1 (8, 9). On the other hand, the proteins belonging to the reticulocyte-binding-like homologue (Rh) protein family, located in the rhoptries, have been shown to translocate and bind to eryth-

Received 1 June 2013 **Returned for modification** 10 July 2013
Accepted 29 August 2013
Published ahead of print 3 September 2013
Editor: J. H. Adams

Address correspondence to Takafumi Tsuboi, tsuboi@ccr.ehime-u.ac.jp.

* Present address: Tsutomu Yamasaki, Department of Life Science, Faculty of Science, Okayama University of Science, Okayama, Japan; Satoru Takeo, Division of Tropical Diseases and Parasitology, Department of Infectious Diseases, Faculty of Medicine, Kyorin University, Mitaka, Tokyo, Japan.

Supplemental material for this article may be found at http://dx.doi.org/10.1128/IAI.00690-13.

doi:10.1128/IAI.00690-13

rocytes, leading to tight-junction formation, and hence play a direct role in invasion (10). In this way, rhoptry proteins might represent promising blood-stage *P. falciparum* vaccine candidates. Therefore, this study was taken up with the objective of characterizing *P. falciparum* rhoptry proteins and assessing them as novel blood-stage vaccine candidates.

Previous bioinformatic searches using transcriptional and structural features of known proteins by Haase et al. (11) have identified hypothetical proteins that are probably located on the surface of the merozoite or in the secretory organelles. Of these candidates, it has been experimentally shown that PF3D7_0722200 appears to be localized in the rhoptry of *P. falciparum* merozoites and to possess a leucine zipper-like domain, a structural feature that facilitates protein-protein interaction, and hence is designated rhoptry-associated leucine zipper-like protein 1 (RALP1). Furthermore, RALP1 is conserved in *Plasmodium* spp. and it is refractory to gene knockout attempts (11), suggesting that RALP1 might play an important role in invasion. However, so far, no studies have attempted growth and/or invasion inhibition assays with antibodies raised against recombinant RALP1 proteins; therefore, RALP1 has yet to be characterized as a vaccine candidate. In this study, we attempted to test whether RALP1 is a potential blood-stage vaccine candidate. In this regard, we expressed recombinant RALP1 by using the wheat germ cell-free system, defined the subcellular localization of RALP1 by immunoelectron microscopy (IEM), tested the growth and/or invasion inhibition activity of anti-RALP1 antibodies, and analyzed the reactivity of malaria immune human sera to RALP1.

MATERIALS AND METHODS

Parasite culture and free-merozoite purification. *P. falciparum* asexual stages (strain 3D7A from the National Institute of Allergy and Infectious Diseases [NIAID], NIH) were maintained *in vitro* in erythrocytes from healthy human donors (blood group O^+) obtained from the Japanese Red Cross Society as described elsewhere (12). To harvest parasite pellets, mature schizonts were purified by differential centrifugation on a 70%/40% Percoll-sorbitol gradient and further treated with tetanolysin (List Biological Laboratories, Inc., Campbell, CA) to remove hemoglobin without loss of parasite proteins present in the PV space (13), washed with phosphate-buffered saline (PBS) containing Complete protease inhibitor (Roche, Mannheim, Germany), and stored at −80°C until used. The viable free merozoites that retain their invasive capacity were purified on the basis of the recently reported protocol (14). Briefly, parasites were synchronized by using sorbitol treatment and heparin (Mochida Pharmaceutical Co., Tokyo, Japan). Late-stage parasites (32 to 36 h postinvasion) were purified (>95% purity) by magnetic separation with a MACS CS column in conjunction with a VarioMACS magnetic separator (Miltenyi Biotec, Cambridge, MA), incubated with 10 μM E64 (Sigma-Aldrich Corporation, St. Louis, MO) for 6 to 8 h, and pelleted. Resulting E64-treated schizonts were resuspended in a small volume of incomplete culture medium (containing no protein component) and filtered through a 1.2-μm Acrodisc 32-mm syringe filter (Pall Corporation, Port Washington, NY).

Production of recombinant proteins and antisera. Genomic DNA was extracted from *P. falciparum* strain 3D7A with the DNAzol reagent (Invitrogen, Carlsbad, CA). The nucleotide sequence of the *ralp1* gene (PF3D7_0722200) of strain 3D7 was obtained from the malaria genome database PlasmoDB (http://plasmodb.org). In order to generate specific antibodies, truncated regions of the *ralp1* gene were amplified and expressed as recombinant proteins with the wheat germ cell-free translation system (CellFree Sciences, Matsuyama, Japan) as described previously (15). Briefly, the PF3D7_0722200 fragments encoding RALP1-N1 (N-terminal region of RALP1, encompassing 114 amino acids [aa; M_{35} to D_{148}] and a hexahistidine tag at the C terminus), RALP1-N2 (N-terminal region of RALP1, encompassing 396 aa [F_{17} to Q_{412}]), RALP1-C1 (C-terminal region of RALP1, encompassing 239 aa [N_{396} to P_{634}]), and RALP1-C2 (C-terminal region of RALP1, encompassing 315 aa [N_{396} to K_{710}]) were amplified from *P. falciparum* 3D7 genomic DNA by PCR by using sense primers with XhoI sites and antisense primers with BamHI restriction sites (in lowercase letters in the primer sequences below). Primers RALP1-N1-F (5′-ctcgagATGCCACTTCAACGTGGCGCATC-3′) and RALP1-N1-R (5′-ggatccCTAGTGATGATGATGATGATGATCA ACGTTCACATTCATTTGTTGATT-3′), primers RALP1-N2-F (5′-ctcga gTTTTACCTGATAAAGTCATCTTCCAAT-3′) and RALP1-N2-R (5′-g gatccCTATTGATCATTCATCAATTTTACAAAAAC-3′), primers RALP1-C1-F (5′-ctcgagAATGGTAAGAAGGATAAAAATGGGGT-3′) and RALP1-C1-R (5′-ggatccCTATGGTACATTTTTAGGTGTAAAAGT AGT-3′), and primers RALP1-C2-F (5′-ctcgagAATGGTAAGAAGGATA AAAATGGGGT-3′) and RALP1-C2-R (5′-ggatccCTATTTGTTTCCCA TATCATTTTTATTATATTT-3′) were used to generate the DNA fragments encoding the RALP1-N1, -N2, -C1, and -C2 proteins, respectively. The underlined sequences in primer RALP1-N1-R indicate the regions that encode the hexahistidine tag.

The amplified fragments were then restricted and ligated into the wheat germ cell-free expression vectors (CellFree Sciences). The fragment encoding RALP1-N1 was cloned into the pEU-E01-MCS vector. Fragments encoding RALP1-N2, -C1, and -C2 were cloned into the pEU-E01-GST-TEV-N2 vector. The cloned inserts were sequenced with an ABI PRISM 3100-Avant genetic analyzer (Applied Biosystems, Foster City, CA). The recombinant proteins with either a His or a glutathione *S*-transferase (GST) tag were expressed with the wheat germ cell-free system and purified with either a nickel-Sepharose column (GE Healthcare) in the case of RALP1-C1 or a glutathione-Sepharose 4B column (GE Healthcare). GST-tagged RALP1-N2 was purified by glutathione elution. In the case of the GST-tagged RALP1-C1 and -C2 proteins, the N-terminal GST tag was removed by eluting GST-tagged RALP1 bound to a glutathione-Sepharose 4B column by using tobacco etch virus (TEV) protease, which cleaves the TEV recognition site between the GST tag and the RALP1 fragment. All of the detailed methods used for wheat germ cell-free protein synthesis and affinity purification were described previously (16).

To generate antisera against each protein (RALP1-N1, -C1, or -C2), two BALB/c mice were immunized subcutaneously with 20 μg of purified recombinant protein emulsified with Freund's complete adjuvant, followed by 20 μg of the protein with Freund's incomplete adjuvant. A Japanese white rabbit was also immunized subcutaneously with 250 μg of purified protein with Freund's complete adjuvant, followed by 250 μg of purified protein with Freund's incomplete adjuvant. All immunizations were done three times at 3-week intervals, and the antisera were collected 14 days after the last immunization. All of the animal experimental protocols were approved by the Institutional Animal Care and Use Committee of Ehime University (su-14-6), and the experiments were conducted according to the Ethical Guidelines for Animal Experiments of Ehime University. In a similar manner, mouse anti-RAP1 (M_1 to D_{782} of the 3D7 sequence [PF3D7_1410400]) antibody, mouse and rabbit anti-AMA1 (Q_{25} to K_{546} of the 3D7 sequence [PF3D7_1133400]) antibodies, and rabbit anti-GST antibody were generated as previously described (17). Mouse anti-RON4 monoclonal antibody (26C64F12) (8) was a kind gift from Jean F. Dubremetz (Université de Montpellier 2, Montpellier, France).

In order to obtain antigen-specific IgGs, rabbit antisera against RALP1 proteins were affinity purified with columns conjugated with respective recombinant RALP1 proteins as ligands. Briefly, recombinant RALP1 proteins were covalently linked to HiTrap NHS-Activated HP columns (GE Healthcare) in accordance with the manufacturer's recommendations. Rabbit antisera were applied to each RALP1 protein-conjugated column. After extensive washing with 20 mM phosphate buffer (pH 7.0), antigen-specific IgGs were eluted with 0.1 M glycine-HCl, pH 2.5, and then immediately neutralized with 1 M Tris, pH 9.0.

Preparation of parasite schizont extract and Western blot analysis. Purified, schizont-rich parasite pellets were lysed in an appropriate amount of reducing SDS-PAGE sample buffer and then incubated at 98°C for 3 min. The lysate was centrifuged at 10,000 × *g* for 10 min at room temperature (RT), and supernatants were subjected to electrophoresis on a 12.5% polyacrylamide gel (ATTO, Tokyo, Japan). Proteins were then transferred to a 0.2-μm polyvinylidene difluoride membrane (Hybond LFP; GE Healthcare) with a semidry blotting system (ATTO). The membranes were blocked with PBS-MT (PBS containing 5% [wt/vol] nonfat milk and 0.1% [vol/vol] Tween 20), and lanes were cut into strips. Then each membrane strip was immunostained with each antiserum at RT for 1 h, followed by horseradish peroxidase-conjugated secondary-antibody (GE Healthcare) probing, and visualized with Immobilon Western chemiluminescent horseradish peroxidase substrate (Millipore, Billerica, MA) on a LAS 4000 Mini luminescent-image analyzer (GE Healthcare). The relative molecular masses of the proteins were estimated with reference to Precision Plus protein standards (Bio-Rad, Hercules, CA).

Imaging of schizont and merozoite invasion by indirect immunofluorescence assay (IFA). Thin smears of schizont-enriched *P. falciparum*-infected erythrocytes were prepared on glass slides and stored at −80°C. The smears were thawed, fixed with 4% paraformaldehyde at RT for 10 min, permeabilized with PBS-T (PBS containing 0.1% Triton X-100) at RT for 15 min, and blocked with PBS containing 5% nonfat milk (blocking solution) at 37°C for 30 min.

Free merozoites were isolated as described above, added to uninfected erythrocytes, and processed for invasion as described previously (14). Invading merozoites were collected after 2 to 10 min of incubation with erythrocytes on a shaker at 37°C, fixed at RT for 30 min with 4% paraformaldehyde–0.0075% glutaraldehyde in PBS, permeabilized with PBS-T at RT for 15 min, blocked with PBS containing 3% bovine serum albumin (BSA) at 37°C for 30 min, and then applied to polyethyleneimine-coated coverslips.

The antigen samples for IFA described above were stained with primary antibodies diluted at the following concentrations in blocking solution at 37°C for 1 h: rabbit anti-RALP1-C1 antibody, 1:500; rabbit anti-RALP1-C2 antibody, 1:500; mouse anti-RALP1-N1 antibody, 1:100; mouse anti-RAP1 antibody, 1:100 (17); mouse anti-RON4 monoclonal antibody, 1:1,000 (gift from Jean F. Dubremetz). Secondary antibodies, Alexa Fluor 488-conjugated goat anti-rabbit IgG and Alexa Fluor 568-conjugated goat anti-mouse IgG (Invitrogen), were used at a 1:500 dilution in blocking solution at 37°C for 30 min. DAPI (4′,6-diamidino-2-phenylindole) at 2 μg/ml was also added to the secondary-antibody solution to stain the nuclei. Slides were mounted in ProLong Gold Antifade reagent (Invitrogen) and viewed under a 63× oil immersion lens. High-resolution image capture and processing were performed with a confocal scanning laser microscope (LSM710; Carl Zeiss MicroImaging, Thornwood, NY). Images were processed in Adobe Photoshop (Adobe Systems Inc., San Jose, CA).

IEM. Parasites were fixed and embedded in LR White resin (Polysciences, Inc., Warrington, PA) as previously described (18). Ultrathin sections were immunostained as previously described (19). Samples were examined with a transmission electron microscope (JEM-1230; JEOL, Tokyo, Japan).

GIAs. Total rabbit IgGs for growth inhibition assays (GIAs) were purified from rabbit antisera with HiTrap protein G-Sepharose columns (GE Healthcare) according to the manufacturer's protocol. Purified IgGs were further buffer exchanged into incomplete culture medium, concentrated with Amicon Ultra-15 centrifugal filter units (Millipore), filter sterilized with an Ultrafree-MC GV 0.22-μm centrifugal filter (Millipore), and preabsorbed to remove nonspecific antierythrocyte antibodies with 25 μl of packed human O^+ erythrocytes per purified IgG from 1 ml of antiserum at RT for 1 h on a rotating wheel. Finally, the concentrations of all rabbit IgG samples were adjusted to 40 mg/ml in incomplete culture medium.

The inhibitory activity of rabbit IgGs on merozoite invasion was tested over one cycle of parasite replication, and parasitemia was determined by flow cytometry as described previously (19). Briefly, the parasite cultures were synchronized the day before the start of the GIA, so that the majority of parasites were at the late trophozoite-to-schizont stage at the start of the GIA. Twenty microliters of parasite-infected erythrocyte (pRBC) suspension (0.3% parasitemia and 2% hematocrit) and 20 μl of IgGs were added per well of half-area flat-bottom 96-well cell culture microplates (Corning, Corning, NY) and gently mixed. For a control, 20 μl of culture medium was added to the pRBC suspension. Cultures were incubated at 37°C in humidified, gassed (90% N_2, 5% O_2, and 5% CO_2), airtight boxes. After 25 h of incubation, when most of the invading parasites had developed to the early trophozoite stage, the pRBC were pelleted by brief centrifugation (1,300 × *g* for 5 min) and washed once in 100 μl PBS. The cells were then incubated with 50 μl of diluted (1:1,000 in PBS) SYBR green I (Invitrogen) for 10 min at RT and washed once in PBS. Parasitemia was measured by flow cytometry with a FACSCanto II (BD Biosciences, San Jose, CA) by the acquisition of 50,000 events per sample. Data were analyzed with FlowJo 9.1 software (Tree Star, Ashley, OR) by first gating for intact erythrocytes by side scatter and forward scatter parameters and subsequently determining the proportion of SYBR green I-positive cells. Samples were tested in triplicate in each experiment, and three independent experiments were performed.

The human IgGs purified from serum samples from Mali were also tested for parasite invasion and growth-inhibitory activity over one cycle of parasite replication at the GIA Reference Center, NIAID, NIH. The GIA reaction mixture was incubated for 40 h in the presence of test IgG to allow most of the invading parasites to develop to the schizont stage, and then parasite growth was determined by a biochemical assay specific for parasite lactate dehydrogenase as previously described (20).

Immunoprecipitation. Immunoprecipitation was carried out as previously described (17). Briefly, proteins were extracted from late schizont parasite pellets in PBS with 1% Triton X-100 containing Complete protease inhibitor. Fifty-microliter samples of supernatants were preincubated at 4°C for 1 h with 40 μl of 50% protein G-conjugated beads (protein G-Sepharose 4 Fast Flow; GE Healthcare) in NETT buffer (50 mM Tris-HCl, 0.15 M NaCl, 1 mM EDTA, 0.5% Triton X-100) supplemented with 0.5% BSA (fraction V; Sigma-Aldrich Corporation). Aliquots of recovered supernatants were incubated with rabbit anti-RALP1-N1, anti-RALP1-C1, anti-AMA1, or anti-GST antibody, and then 40 μl of a 50% protein G-conjugated bead suspension was added. After incubation for 1 h at 4°C, the beads were washed once with NETT–0.5% BSA, once with NETT, once with high-salt (0.5 M NaCl) NETT, once with NETT, and once with low-salt (0.05 M NaCl, 0.17% Triton X-100) NETT. Finally, proteins were extracted from the protein G-conjugated beads by incubation with 1× SDS-PAGE reducing loading buffer at 98°C for 3 min. The supernatants were used for Western blot analysis.

FACS-based EBA. An assay for checking the erythrocyte-binding activity of RALP1 was done on the basis of a protocol used to assay the erythrocyte-binding activity of Duffy antigen (21). Rh5 of *P. falciparum* is unique among the erythrocyte-binding proteins because it cannot be deleted from any *P. falciparum* strain. Both native and recombinant Rh5 have previously been shown to bind erythrocytes (22). Therefore, we used Rh5 as a universal positive-control protein in an erythrocyte-binding assay (EBA). In brief, GST-tagged RALP1-N2, RALP1-C1, full-length Rh5 (comprising aa E_{26} to Q_{526} of the 3D7 sequence [PF3D7_0424100] without the signal peptide), and GST (negative control) were synthesized by the wheat germ cell-free system and purified by glutathione-Sepharose column chromatography with glutathione elution as described above. Erythrocytes were washed three times with PBS–1% BSA, resuspended to 1×10^5 cells in 200 μl of PBS–1% BSA, and then preincubated with 20 μg recombinant protein at RT for 3 h. After preincubation, erythrocytes were washed with PBS once and then incubated with fluorescein isothiocyanate (FITC)-conjugated anti-GST antibody (1:100 in PBS with 1% BSA; Abcam, Cambridge, United Kingdom) at RT for 1 h while protected from light. Erythrocytes were washed with PBS once, resuspended in 200 μl of PBS, and transferred to fluorescence-activated cell sorter (FACS) tubes. A

total of 50,000 erythrocytes were read on a FACSCanto II flow cytometer, and the resulting flow cytometry data were analyzed with FlowJo software. The percentage of erythrocytes with bound recombinant RALP1 (% of cells) was obtained from the percentage of erythrocytes with a positive FITC signal above the background FITC measurement of erythrocytes without any recombinant protein.

IFA-based MIBA. Total IgGs to be tested in a merozoite invasion-blocking assay (MIBA) were purified from rabbit antisera as described above. To the filtered merozoites, antibodies were added at a final concentration of 20 mg/ml of total IgG of anti-RALP1-C1 or anti-GST serum (diluted in incomplete culture medium) and uninfected erythrocytes (50% hematocrit; 10 μl) and incubated at 37°C for 10 min. Control assays were performed with incomplete culture medium. After fixation and washing, samples were processed for IFA with DAPI and mouse anti-RAP1 antibody as described above. For each condition, three biological replicates of approximately 2,000 erythrocytes with attached or invading parasites were scored under a confocal scanning laser microscope.

ELISAs. Human serum samples from western Thailand were collected from asymptomatic *P. falciparum* carriers with written informed consent as previously described (23). The study was approved by the Ethics Committee of the Thai Ministry of Public Health and the Institutional Review Board of the Walter Reed Army Institute of Research (WRAIR number 802) (23). Human serum samples were also collected from adults living in the village of Kenieroba, Mali (24). The study was approved by the ethical review committees of the Faculty of Medicine, Pharmacy, and Dentistry at the University of Bamako (Mali) and the NIAID, National Institutes of Health, Bethesda, MD (NIAID protocol number 08-I-N120). Individual written informed consent was obtained from all participants. Measurements of antibodies against recombinant RALP1-C1 in the 1:1,000-diluted Thai or Mali sera were performed as previously described (24). The enzyme-linked immunosorbent assays (ELISAs) were replicated twice independently.

Statistical analysis. The Mann-Whitney U test was used to test the significance of differences in ELISA values between groups, and Spearman's rank correlation test was used to test the correlation between ELISA and GIA values. For GIA and EBA data, the Kruskal-Wallis test was used, followed by Dunn's multiple-comparison test to examine the differences between negative-control- and experimental-group values. For MIBA, Fisher's exact test with Bonferroni correction was performed. All statistical analyses were performed with GraphPad Prism (GraphPad Software, San Diego, CA).

RESULTS

RALP1 is localized at the merozoite rhoptry neck. In order to characterize RALP1, we produced recombinant RALP1 proteins (Fig. 1A without codon optimization. Figure 1B shows the different truncated RALP1 proteins, RALP1-N1 (predicted molecular mass, 13.9 kDa), RALP1-C1 (27.5 kDa), RALP1-N2 (fused with GST, 76.0 kDa), and RALP1-C2 (37.4 kDa), resolved in a 12.5% SDS-polyacrylamide gel and stained with Coomassie brilliant blue R-250. N1, C1, and C2 truncated versions of the RALP1 protein were recovered in the supernatant fraction and easily purified as single dominant bands (Fig. 1B, arrowheads) by affinity chromatography. Since the electrophoretic mobility of the N1, C1, and C2 proteins (Fig. 1B, arrowhead) is slower, their observed molecular masses are higher than their predicted molecular masses. Even though RALP1-N2 was derived as multiple bands, a full-length band with slightly faster electrophoretic mobility was clearly seen (Fig. 1B, arrowhead). The appearance of smaller bands of N2 proteins (Fig. 1B, asterisks) may be caused by the translational arrest during the reaction, because all of those smaller bands retain the GST tag at the N terminus (data not shown). These results demonstrate that the wheat germ cell-free system is able to translate the native RALP1-encoding gene sequences and produce soluble proteins. The N1, C1, and C2 truncated proteins were used to immunize rabbits and mice to produce antibodies.

RALP1 expression was analyzed with RALP1-specific antibodies in a Western blot assay of protein extracts of synchronized schizont-rich parasites. All of the antisera raised against the N1, C1, and C2 truncated forms of RALP1 recognized a protein of >90 kDa in protein extracts from *P. falciparum* parasites in schizont stages (Fig. 1C, arrowhead), corresponding to the predicted molecular mass of 88 kDa. Additionally, anti-RALP1-N1 and both anti-RALP1-C1 and anti-RALP1-C2 antisera recognized distinct 53- and 50-kDa proteins, respectively, that represent processed N- and C-terminal forms of the RALP1 protein (Fig. 1C, asterisks). In the case of anti-RALP1-C1 and -C2 antiserum staining, a faint band around 40 kDa is visible, suggesting a further processing event in the C-terminal region of RALP1. The negative-control lane stained only with the secondary antibody showed no signal (Fig. 1C, Ctrl), indicating that the signals described above were specific.

In order to confirm the exact localization of RALP1 within merozoite rhoptries, we used antisera against RAP1, a rhoptry bulb marker, and RON4, a rhoptry neck marker, to test if RALP1 resides in one of these compartments by IFA (Fig. 1D). The IFA results showed that the apical distribution of RALP1, detected with anti-RALP1-C2 antiserum, is clearly the same as that of RON4 (Fig. 1D, middle) and not that of RAP1 (Fig. 1D, top). Furthermore, the distribution of RALP1 detected with anti-RALP1-C2 antiserum overlaps that of RALP1 detected with anti-RALP1-N1 antiserum (Fig. 1D, bottom). IFA with anti-RALP1-C1 antiserum also shows that RALP1 colocalizes with RON4 (see Fig. S1 in the supplemental material).

To further validate the precise subcellular localization of RALP1 in the merozoite by electron microscopy, parasites in late schizont stages were stained with RALP1-C2 specific IgG and subsequently with a secondary antibody labeled with gold particles. Gold particle signals were detected in the neck portion of the rhoptries of merozoites (Fig. 1E). Together, these findings establish that RALP1 is a novel RON of merozoites.

RALP1 translocates to the moving junction during merozoite invasion. The data from another study (11) supporting a direct role for RALP1 in parasite invasion are limited. It is clear from our data that RALP1 is expressed at the rhoptry neck of the merozoite and that antibodies to it inhibit merozoite invasion. Recent studies have shown that both RONs and Rhs are part of the tight-junction proteins, suggesting a specific role for RONs during this part of the invasion process (10, 25). To investigate the role of RALP1 during merozoite invasion of erythrocytes, we performed IFA and analyzed the localization of RALP1 with reference to rhoptry neck and bulb markers (RON4 and RAP1), which have been shown previously to localize in the tight junction and the PV, respectively, during merozoite invasion (26). By using invading merozoites, we showed by confocal microscopic examination that RALP1 colocalized with RON4 at the moving junction throughout the invasion process (Fig. 2A). Figure 2B shows that RAP1 fluorescence is seen surrounding the parasite at the PV at late invasion stages. However, RALP1 fluorescence was observed not in the PV but only at the posterior end of the parasite (Fig. 2B). Taken together, these observations indicate that RALP1 is a tight-junction protein and suggest that RALP1 could play an important role in merozoite invasion of erythrocytes.

RALP1 does not interact with AMA1. To investigate whether RALP1 interacts with the well-known RON-AMA1 moving-junc-

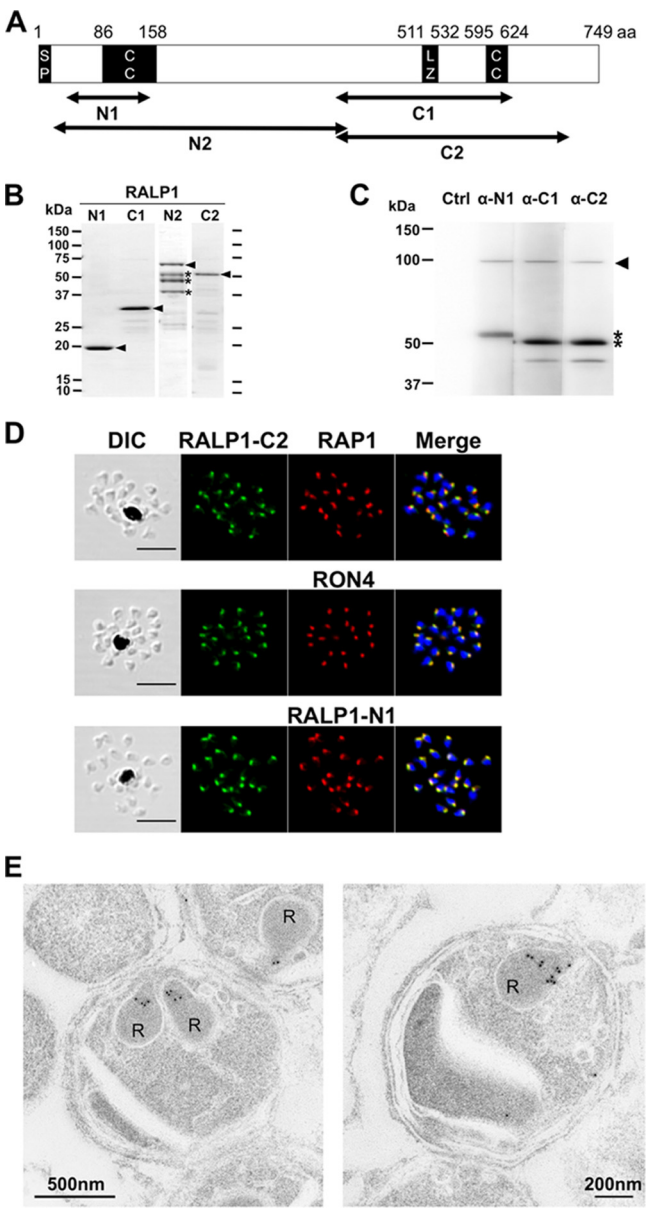

FIG 1 Structure, expression, and localization of RALP1 in *P. falciparum* merozoites. (A) Schematic of the primary structure of RALP1. The RALP1 protein consists of 749 aa with a calculated molecular mass of 87.9 kDa. The predicted signal peptide (SP; residues 1 to 17), leucine zipper-like domain (LZ; residues 511 to 532), and coiled-coil domain (CC; residues 86 to 158 and 595 to 624) are indicated. RALP1-N1 (residues 35 to 148), RALP1-N2 (residues 17 to 412), RALP1-C1 (residues 396 to 634), and RALP1-C2 (residues 396 to 710) were expressed as recombinant proteins, and antibodies were raised against RALP1-N1, RALP1-C1, and RALP1-C2. (B) SDS-PAGE of recombinant RALP1 proteins. All of the recombinant RALP1 proteins were synthesized with the wheat germ cell-free protein expression system and purified with affinity purification columns. The fractions of purified RALP1-N1 (predicted molecular mass, 13.9 kDa), RALP1-C1 (27.5 kDa), RALP1-N2 (fused with GST, 76.0 kDa), and RALP1-C2 (37.4 kDa) proteins resolved by 12.5% SDS-PAGE and stained with Coomassie brilliant blue R-250 are shown. Arrowheads indicate bands of full-length proteins. Asterisks represent bands of truncated N2 proteins. (C) Detection of RALP1 in schizont lysate. Total schizont material was examined by Western blotting under reducing condition with rabbit anti-RALP1-N1 (α-N1), anti-RALP1-C1 (α-C1), and anti-RALP1-C2 (α-C2) antisera. The arrowhead indicates full-length RALP1, and the asterisks indicate the processed N- and C-terminal forms of the RALP1 protein. (D) RALP1 localization shown by an immunofluorescence assay. Paraformaldehyde-fixed mature schizonts were probed with rabbit anti-RALP1-C2 (green) and mouse anti-RAP1 (rhoptry bulb marker) antibodies (top) or anti-RON4 (rhoptry neck marker) (middle) or anti-RALP1-N1 (bottom) (red) antibody. Parasite nuclei were stained with DAPI (blue). Scale bars represent 5 μm. DIC, differential interference contrast. (E) RALP1 localization shown by IEM. Two sections of merozoites in schizont-infected erythrocytes probed with purified rabbit anti-RALP1-C2 antibody and subsequently with a secondary antibody conjugated with gold particles are shown. The black dots indicate signals from gold particles localized in rhoptry necks. R, rhoptry.

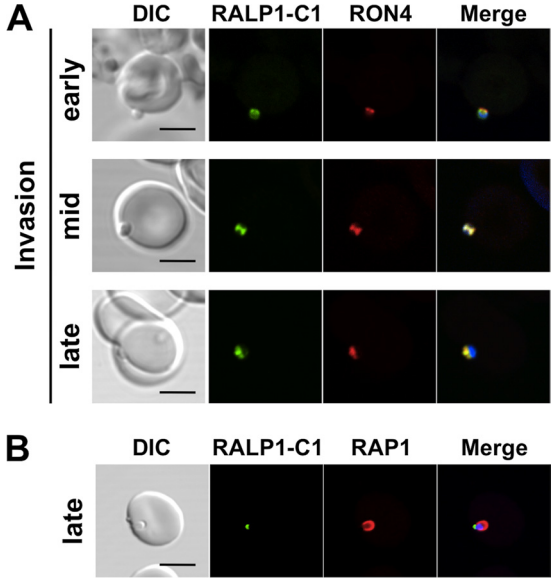

FIG 2 RALP1 is localized at the moving junction during invasion. RALP1 colocalizes with the moving-junction marker (RON4) from the early through the mid and late stages of invasion (A). RAP1 is used as a PV marker (B). Scale bars represent 5 μm. DIC, differential interference contrast.

tion complex, we performed coimmunoprecipitation experiments with anti-RALP1 and anti-AMA1 antibodies and mature-schizont-rich parasite extracts. Immunoprecipitation with either anti-RALP1-N1 or anti-RALP1-C1 antibodies, to pull down RALP1 from schizont lysates, brought down both full-length RALP1 protein (approximately 90 kDa) and the processed RALP1 fragment (approximately 50 kDa) but not AMA1 or RON4 (Fig. 3). The reciprocal experiment, in which we immunoprecipitated AMA1 with the anti-AMA1 antibody, pulled down both AMA1 and RON4 as a control for the RON-AMA1 complex but not RALP1. As a negative control, no proteins were detected in an immunoprecipitation experiment with anti-GST antibody (Fig. 3).

RALP1 binds to human erythrocytes through its C-terminal region. Since the RALP1 protein possesses three coiled-coil domains, including a leucine zipper-like domain that might represent a protein-protein interaction domain (Fig. 1A), and is localized at a moving junction (Fig. 2), we investigated whether RALP1 binds to human erythrocytes. While it was preferable to use native parasite RALP1 protein, Haase et al. (11) have previously reported that RALP1 was not detectable in parasite culture supernatants and RALP1 appears to partition into the insoluble fraction of the late-stage parasite lysate (more than 50%), even though it does not contain a predicted transmembrane domain or GPI anchor signal. Therefore, we used recombinant GST-tagged RALP1 proteins for

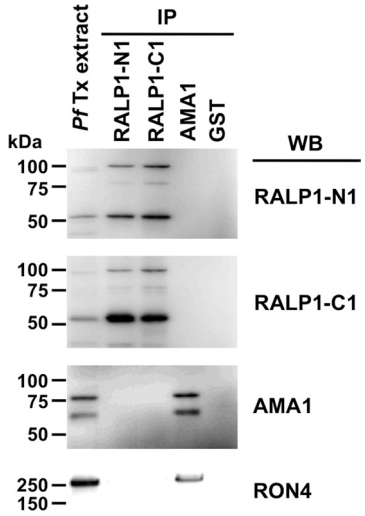

FIG 3 RALP1 does not interact with the RON-AMA1 complex. Triton X-100 extracts of schizont-rich parasite (*Pf*Tx extract) were immunoprecipitated (IP) with rabbit serum against RALP1-N1, RALP1-C1, AMA1, or GST and then detected by Western blotting (WB) with mouse antiserum against RALP1-N1, RALP1-C1, AMA1, or RON4. Immunoprecipitation with anti-GST antibody was used as a negative control. No bands were detected in the anti-GST immunoprecipitate.

the EBA. The EBA was performed with glutathione affinity-purified, GST-tagged Rh5, RALP1-N2, RALP1-C1, and GST (Fig. 4A). As shown in Fig. 1C, RALP1 undergoes processing by cleavage in its middle portion; however, the precise cleavage site of RALP1 is

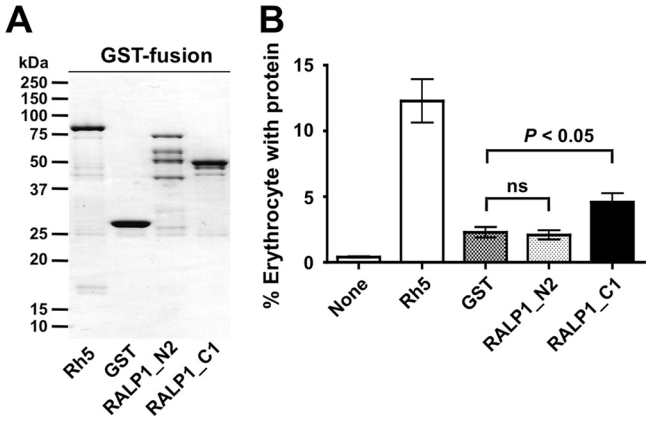

FIG 4 EBA with recombinant RALP1. (A) SDS-PAGE of recombinant proteins used for EBA. All of the recombinant proteins were synthesized with the wheat germ cell-free protein expression system as GST fusion proteins and purified with affinity purification columns. The fractions of purified, GST-tagged Rh5 (87 kDa), GST (27 kDa), RALP1-N2 (76 kDa), and RALP1-C1 (55 kDa) proteins resolved by SDS-PAGE and stained with Coomassie brilliant blue R-250 are shown. (B) Erythrocyte-binding activities of recombinant RALP1 proteins. The GST-tagged recombinant proteins were incubated with human erythrocytes. Then the recombinant proteins bound to erythrocytes were stained with FITC-conjugated anti-GST antibody. The labeled erythrocytes were counted by flow cytometry. As a control, erythrocytes in the absence of any recombinant proteins were also counted by flow cytometry (None). The vertical axis represents the mean percentage of erythrocytes with bound recombinant protein calculated from nine independent experiments. The error bars indicate the standard errors of the means of nine independent experiments. The Kruskal-Wallis test was performed, followed by Dunn's multiple-comparison test, to compare the means of the GST and RALP1-N2 groups or the GST and anti-RALP1-C1 groups. ns, not significant.

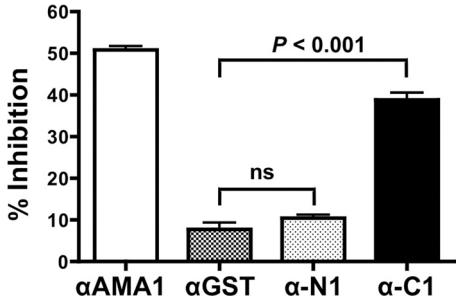

FIG 5 Anti-RALP1-C1 antibody has invasion-inhibitory activity *in vitro*. The ability of the anti-RALP1-N1 (α-N1) and anti-RALP1-C1 (α-C1) antibodies to inhibit the parasite invasion of erythrocytes was tested in a one-cycle GIA. Anti-AMA1 (αAMA1) and anti-GST (αGST) antibodies were used as positive and negative controls, respectively. The error bars represent the standard errors of the means of three independent experiments. The Kruskal-Wallis test was performed, followed by Dunn's multiple-comparison test, to compare percent inhibition by anti-GST and anti-RALP1-N1 antibodies or anti-GST and anti-RALP1-C1 antibodies. ns, not significant.

still unknown. Considering that there might be an erythrocyte-binding epitope in the middle region of RALP1, we designed RALP1-N2, which overlaps the N terminus of RALP1-C1 by 17 aa residues (i.e., N_{396} to Q_{412}). The erythrocyte-binding activity of RALP1-C1 (mean ± the standard error of the mean [SEM], 4.6% ± 0.7%) was significantly higher than that of the negative control, GST (2.3% ± 0.4%) ($P < 0.05$). The binding activity of RALP1-N2 was similar to that of GST (Fig. 4B). These results suggest that RALP1 has an erythrocyte-binding epitope in the C-terminal region and that RALP1 is a new erythrocyte-binding protein of *P. falciparum*.

Antibodies to RALP1-C1 inhibit merozoite invasion. In order to test whether antibodies to RALP1 could block parasite invasion, rabbit polyclonal IgGs to RALP1-N1 and -C1 were tested for inhibition of parasite growth over one cycle of replication with measurement of parasite growth by flow cytometry. When anti-RALP1-N1, anti-RALP1-C1, anti-AMA1 (positive control), and anti-GST (negative control) antibodies were tested at a final concentration of 20 mg/ml (total IgG concentration), they inhibited invasion by (mean ± SEM) 10% ± 0.8%, 39% ± 1.6%, 51% ± 0.9%, and 7.8% ± 1.6%, respectively (Fig. 5). The invasion-inhibiting activity of anti-RALP1-C1 antibody was significantly higher than that of the negative-control anti-GST antibody ($P < 0.001$). Anti-RALP1-N1 antibody did not show significant inhibition activity, and its inhibition activity was as negligible as that of the anti-GST antibody.

Anti-RALP1 antibodies cause merozoites to aberrantly release RAP1 in an IFA-based MIBA. To understand more about the mechanism of invasion inhibition by anti-RALP1-C1 antibody in the GIA, we performed a MIBA that evaluates, by IFA inspection, the efficiency with which isolated viable, invasion-competent merozoites invade erythrocytes in the presence of antibodies. In order to count parasites invading erythrocytes and to distinguish between pre- and postinvasion merozoites, an IFA was performed with DAPI labeling as a nuclear marker and RAP1 labeling as a PV marker. Figure 6A shows different states of RAP1 release during merozoite invasion of erythrocytes: state 1, RAP1 unreleased (i.e., yet to be released); state 2, RAP1 properly released into the PV; state 3, RAP1 aberrantly released onto the erythrocyte or merozoite surface. As an untreated control, we per-

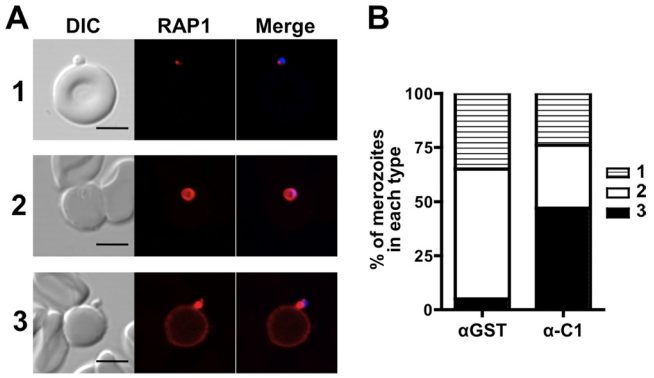

FIG 6 Anti-RALP1 antibody causes merozoites to aberrantly release RAP1 in a MIBA. (A) Imaging of erythrocyte-associated merozoites stained with anti-RAP1 antibody and DAPI for analysis of RAP1 localization during invasion in the presence of anti-RALP1-C1 antibody. Merozoites were categorized into three types based on their RAP1 staining patterns: 1, RAP1 unreleased; 2, RAP1 properly released into the PV; 3, RAP1 aberrantly released onto the erythrocyte or merozoite surface. The scale bars represent 5 μm. DIC, differential interference contrast. (B) Stacked bar graph comparing the mean percentages of merozoites of types 1 to 3 (shown in panel A) in the presence of anti-GST (αGST) or anti-RALP1-C1 (α-C1) antibody.

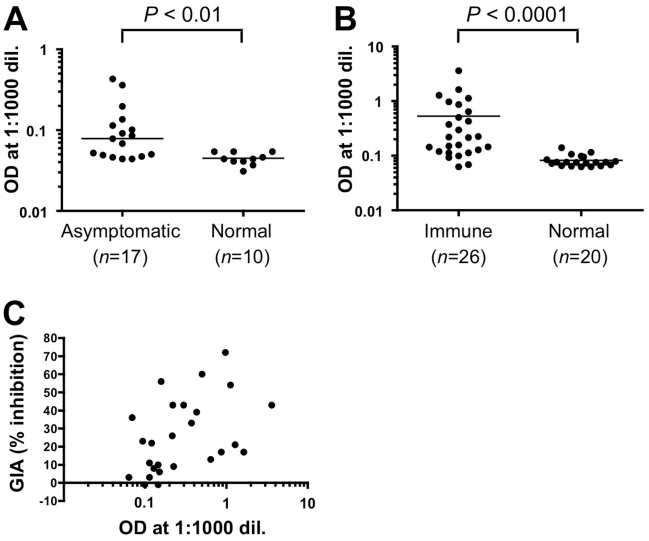

FIG 7 Human sera from areas of Thailand and Mali where malaria is endemic recognize RALP1 in an ELISA. Probing of RALP1-C1 with sera from *P. falciparum*-infected asymptomatic Thai adults (Asymptomatic) and naive, nonexposed Thai adults (Normal) (A) and with sera from semi-immune adults in Mali (Immune) and naive, nonexposed U.S. adults (Normal) (B). *P* values were calculated by Mann-Whitney U test. The number (*n*) of serum samples analyzed is shown. (C) Correlation between anti-RAPL1-C1 antibody titers (logarithmic scale) and *in vitro* growth-inhibitory activities of the Mali semi-immune serum samples. The graph shows a significant positive correlation between antibody titers and growth-inhibitory activities (Spearman's rank correlation, $r = 0.51$; 95% confidence interval, 0.14 to 0.75; $P < 0.01$). OD, optical density; dil., dilution.

formed a MIBA with incomplete culture medium without any antibodies. There was no significant difference observed between the total number of merozoites associated with untreated erythrocytes and that associated with erythrocytes treated with either anti-GST antibody (mean ± SEM, 108% ± 5% of the untreated-control value) or anti-RALP1-C1 antibody (112% ± 5%). Furthermore, the proportion of parasites with unreleased RAP1 (Fig. 6A, state 1) observed in the presence of anti-RALP1-C1 (α-C1) antibody was not significantly different (Fisher's exact test adjusted $P = 0.48$) from that observed in the presence anti-GST (αGST) antibody (Fig. 6B, state 1).

However, the proportion of merozoites that had invaded (Fig. 6A, state 2) (measured by counting properly secreted RAP1 staining) was significantly reduced by anti-RALP1-C1 antibody compared to anti-GST antibody (Fisher's exact test adjusted $P < 0.001$) (Fig. 6B, state 2). Importantly, the proportion of merozoites that released RAP1 aberrantly (Fig. 6A, state 3) was significantly higher in the presence of anti-RALP1-C1 antibody than in the presence of control anti-GST antibody (Fisher's exact test adjusted $P < 0.001$) (Fig. 6B, state 3). Samples were tested in triplicate in each experiment. Two more independent experiments were performed (see Fig. S2 in the supplemental material), and these results are in agreement with those in Fig. 6B. In short, these results suggest that anti-RALP1 antibody affects merozoite invasion of erythrocytes but not merozoite attachment to erythrocytes.

Reactivity of RALP1 to human immune sera. Since anti-RALP1 antibodies inhibited merozoite invasion *in vitro* (Fig. 5 and 6B), we decided to investigate whether RALP1 is exposed to the human immune system in *P. falciparum*-infected individuals and generates an immune response. In order to test for the presence of anti-RALP1 antibody in the sera, we tested sera from *P. falciparum*-infected asymptomatic adults in western Thailand and naive, nonexposed Thai adults for antibodies to RALP1-C1 recombinant protein by ELISA (Fig. 7A) and sera from semi-immune adults from Mali, in western Africa, and naive, nonexposed U.S. adults for antibodies to RALP1-C1 recombinant protein (Fig. 7B). Sera of asymptomatic Thai adults (asymptomatic) showed significantly higher reactivity to RALP1-C1 than those of malaria-naive Thai individuals (normal) ($P < 0.01$, Mann-Whitney U test) (Fig. 7A), and sera of semi-immune adults from Mali (Immune) showed significantly higher reactivity to RALP1-C1 than those of malaria-naive U.S. adults (normal) ($P < 0.01$, Mann-Whitney U test) (Fig. 7B). We also evaluated the functional activity of purified IgGs from the Malian sera against *P. falciparum* 3D7 parasites in an *in vitro* GIA to investigate a correlation between antibody titer against RAPL1-C1 and *in vitro* growth-inhibitory activity. As shown in Fig. 7C, there is a significant positive correlation between antibody titer and growth-inhibitory activity (Spearman's rank correlation, $r = 0.51$; 95% confidence interval, 0.14 to 0.75; $P < 0.01$). Taken together, these results suggest that RALP1 is immunogenic during malaria infection in humans.

DISCUSSION

RALP1 of *P. falciparum* was previously found to be specifically expressed in schizont stages and localized to the rhoptry of merozoites on the basis of IFA. It has also been refractory to gene knockout attempts, suggesting that RALP1 is essential for blood-stage parasite survival; however, RAPL1 has yet to be experimentally characterized as a vaccine candidate. Here, we aimed to characterize RALP1 of *P. falciparum* as a blood-stage vaccine candidate by using recombinant RALP1 expressed in the wheat germ cell-free system.

Our Western blotting results (Fig. 1C) are in agreement with the previous report (11) that primary processing events occur in RALP1. In addition, our IEM results (Fig. 1E) have confirmed for the first time that RALP1 is indeed localized in the merozoite

rhoptry neck, and hence, RALP1 represents a novel RON. Furthermore, our IFA results obtained with merozoites invading erythrocytes (Fig. 2) revealed that RALP1 translocates to the moving junction during invasion and hence RALP1 is a novel tight-junction protein. Since RALP1 is a tight-junction protein, we expected that RALP1 might be a component of the RON-AMA1 complex. However, our immunoprecipitation results showed that neither AMA1 nor RON4 could be immunoprecipitated with RALP1, suggesting that RALP1 is not part of the RON-AMA1 complex (Fig. 3). The fact that RALP1 is a novel tight-junction protein (Fig. 2) with an erythrocyte-binding epitope in the C-terminal region (Fig. 4) suggests that RALP1 plays a role as a bridging protein between the erythrocyte surface and the merozoite surface. However, the lack of a transmembrane region in RALP1 (Fig. 1A) suggests that RALP1 might be associated with an unknown membrane protein anchored to the merozoite surface and that RALP1 plays a role as an invasion ligand, as well as Rh proteins (10, 27). Therefore, further studies are required to find the RALP1 receptor on the erythrocyte membrane and possible merozoite surface proteins that anchor RALP1 on the parasite surface.

GIA and MIBA measure the capacity of antibodies to limit parasite growth and/or invasion of *P. falciparum in vitro* (28). Our GIA and MIBA results show that anti-RALP1 antibodies specifically inhibited the invasion of erythrocytes by merozoites but not the attachment of merozoites to erythrocytes. Our MIBA results clearly show that anti-RALP1 antibody caused more merozoites to aberrantly release RAP1 onto the merozoite or erythrocyte surface and not into the host cell than the negative control did, suggesting that RALP1 plays an important role in correct tight-junction formation and the normal release of RAP1 into the host cell. The aberrant RAP1 release observed in our study is akin to that previously described as abortive merozoite invasion and anomalous premature rhoptry bulb release during merozoite invasion in the presence of the R1 inhibitory peptide that blocks the formation of the RON-AMA1 complex (26). Our data are consistent with the previous finding (26) that rhoptry bulb release and correct tight-junction formation occur independently but are triggered only after committed merozoite attachment—an event likely initiated by erythrocyte-binding-like/Rh proteins (26).

Immunoreactive antigens involved in erythrocyte invasion represent potential candidates for malaria vaccine (29), and designing a vaccine based on sequences of immunoreactive antigens with minimum polymorphisms is critical to preventing the parasite from evading vaccine-induced immunity. Not only do our GIA results (Fig. 5) indicate that antibodies against RALP1-C1 have invasion-inhibitory activity, but our immunoscreening results (Fig. 7) also demonstrate that there is a significant correlation between the reactivity of the Mali semi-immune sera against RAPL1-C1 and *in vitro* growth-inhibitory activity, suggesting that RALP1-C1 contains the invasion-inhibitory epitope and correlates with immunity in humans developed following natural infection in areas where malaria is endemic.

Previous preliminary single nucleotide polymorphism (SNP) analyses suggested that RALP1 is less polymorphic (11). In order to study whether the region of RALP1-C1 is exposed to host immune pressure, we compared the SNPs in RALP1 of 14 laboratory strains (see Table S1 in the supplemental material) deposited in PlasmoDB. This SNP analysis revealed that RALP1 contains a total of nine nonsynonymous SNPs, and all of them are within the RALP1-C1 region (residues 396 to 634 in Fig. 1A); however, they reside outside the leucine zipper-like domain (residues 511 to 532 in Fig. 1A) and coiled-coil domain (residues 595 to 624 in Fig. 1A) of RALP1. These preliminary SNP analyses suggest that the leucine zipper-like domain and the coiled-coil domain of RAPL1 are essential for the function of this protein. However, to validate this claim, we need further analysis of SNPs of RALP1 in different field isolates worldwide.

Overall, our findings indicate that RALP1 is a novel rhoptry neck erythrocyte-binding blood-stage antigen of *P. falciparum* merozoites, and it is an immunogenic antigen in humans that might be a target of antibodies that contribute to acquired immunity to falciparum malaria. Therefore, RALP1 might be a potential blood-stage vaccine candidate antigen of *P. falciparum*. This study also substantiates our claims that the wheat germ cell-free system is a valuable tool for the identification of novel malaria vaccine candidates.

ACKNOWLEDGMENTS

We are grateful to the adults from Kenieroba, Mali, who donated sera, and we appreciate the efforts of Rick Fairhurst, Mahamadou Diakite, Jennifer Anderson, and Saibou Doumbia in facilitating the availability of the sera. We are also grateful to Jean F. Dubremetz for anti-RON4 monoclonal antibody. We thank Masachika Shudo, Integrated Center for Science, Ehime University, Japan for technical assistance. We also thank the Japanese Red Cross Society for providing human erythrocytes and human plasma.

This work was supported in part by MEXT KAKENHI (23117008) and JSPS KAKENHI (23406007) in Japan and a grant from the Ministry of Health, Labor, and Welfare (H21-Chikyukibo-ippan-005), Japan. The study with Malian samples was supported by the intramural program of the NIAID, NIH, and by the PATH Malaria Vaccine Initiative.

REFERENCES

1. **WHO.** 2011. World malaria report 2011. WHO Press, Geneva, Switzerland.
2. **Crompton PD, Pierce SK, Miller LH.** 2010. Advances and challenges in malaria vaccine development. J. Clin. Invest. **120:**4168–4178.
3. **Greenwood BM, Targett GA.** 2011. Malaria vaccines and the new malaria agenda. Clin. Microbiol. Infect. **17:**1600–1607.
4. **Birkett AJ.** 2010. PATH Malaria Vaccine Initiative (MVI): perspectives on the status of malaria vaccine development. Hum. Vaccin. **6:**139–145.
5. **Cowman AF, Crabb BS.** 2006. Invasion of red blood cells by malaria parasites. Cell **124:**755–766.
6. **Iyer J, Gruner AC, Renia L, Snounou G, Preiser PR.** 2007. Invasion of host cells by malaria parasites: a tale of two protein families. Mol. Microbiol. **65:**231–249.
7. **Preiser P, Kaviratne M, Khan S, Bannister L, Jarra W.** 2000. The apical organelles of malaria merozoites: host cell selection, invasion, host immunity and immune evasion. Microbes Infect. **2:**1461–1477.
8. **Alexander DL, Arastu-Kapur S, Dubremetz JF, Boothroyd JC.** 2006. *Plasmodium falciparum* AMA1 binds a rhoptry neck protein homologous to TgRON4, a component of the moving junction in *Toxoplasma gondii*. Eukaryot. Cell **5:**1169–1173.
9. **Cao J, Kaneko O, Thongkukiatkul A, Tachibana M, Otsuki H, Gao Q, Tsuboi T, Torii M.** 2009. Rhoptry neck protein RON2 forms a complex with microneme protein AMA1 in *Plasmodium falciparum* merozoites. Parasitol. Int. **58:**29–35.
10. **Gunalan K, Gao X, Yap SS, Huang X, Preiser PR.** 2013. The role of the reticulocyte-binding-like protein homologues of *Plasmodium* in erythrocyte sensing and invasion. Cell. Microbiol. **15:**35–44.
11. **Haase S, Cabrera A, Langer C, Treeck M, Struck N, Herrmann S, Jansen PW, Bruchhaus I, Bachmann A, Dias S, Cowman AF, Stunnenberg HG, Spielmann T, Gilberger TW.** 2008. Characterization of a conserved rhoptry-associated leucine zipper-like protein in the malaria parasite *Plasmodium falciparum*. Infect. Immun. **76:**879–887.
12. **Trager W, Jensen JB.** 1976. Human malaria parasites in continuous culture. Science **193:**673–675.

13. **Hiller NL, Akompong T, Morrow JS, Holder AA, Haldar K.** 2003. Identification of a stomatin orthologue in vacuoles induced in human erythrocytes by malaria parasites. A role for microbial raft proteins in apicomplexan vacuole biogenesis. J. Biol. Chem. **278:**48413–48421.
14. **Boyle MJ, Wilson DW, Richards JS, Riglar DT, Tetteh KK, Conway DJ, Ralph SA, Baum J, Beeson JG.** 2010. Isolation of viable *Plasmodium falciparum* merozoites to define erythrocyte invasion events and advance vaccine and drug development. Proc. Natl. Acad. Sci. U. S. A. **107:**14378–14383.
15. **Tsuboi T, Takeo S, Iriko H, Jin L, Tsuchimochi M, Matsuda S, Han ET, Otsuki H, Kaneko O, Sattabongkot J, Udomsangpetch R, Sawasaki T, Torii M, Endo Y.** 2008. Wheat germ cell-free system-based production of malaria proteins for discovery of novel vaccine candidates. Infect. Immun. **76:**1702–1708.
16. **Tsuboi T, Takeo S, Sawasaki T, Torii M, Endo Y.** 2010. An efficient approach to the production of vaccines against the malaria parasite. Methods Mol. Biol. **607:**73–83.
17. **Ito D, Han ET, Takeo S, Thongkukiatkul A, Otsuki H, Torii M, Tsuboi T.** 2011. Plasmodial ortholog of *Toxoplasma gondii* rhoptry neck protein 3 is localized to the rhoptry body. Parasitol. Int. **60:**132–138.
18. **Aikawa M, Atkinson CT.** 1990. Immunoelectron microscopy of parasites. Adv. Parasitol. **29:**151–214.
19. **Arumugam TU, Takeo S, Yamasaki T, Thonkukiatkul A, Miura K, Otsuki H, Zhou H, Long CA, Sattabongkot J, Thompson J, Wilson DW, Beeson JG, Healer J, Crabb BS, Cowman AF, Torii M, Tsuboi T.** 2011. Discovery of GAMA, a *Plasmodium falciparum* merozoite micronemal protein, as a novel blood-stage vaccine candidate antigen. Infect. Immun. **79:**4523–4532.
20. **Malkin EM, Diemert DJ, McArthur JH, Perreault JR, Miles AP, Giersing BK, Mullen GE, Orcutt A, Muratova O, Awkal M, Zhou H, Wang J, Stowers A, Long CA, Mahanty S, Miller LH, Saul A, Durbin AP.** 2005. Phase 1 clinical trial of apical membrane antigen 1: an asexual blood-stage vaccine for *Plasmodium falciparum* malaria. Infect. Immun. **73:**3677–3685.
21. **Tran TM, Moreno A, Yazdani SS, Chitnis CE, Barnwell JW, Galinski MR.** 2005. Detection of a *Plasmodium vivax* erythrocyte binding protein by flow cytometry. Cytometry A **63:**59–66.
22. **Baum J, Chen L, Healer J, Lopaticki S, Boyle M, Triglia T, Ehlgen F, Ralph SA, Beeson JG, Cowman AF.** 2009. Reticulocyte-binding protein homologue 5—an essential adhesin involved in invasion of human erythrocytes by *Plasmodium falciparum*. Int. J. Parasitol. **39:**371–380.
23. **Coleman RE, Kumpitak C, Ponlawat A, Maneechai N, Phunkitchar V, Rachapaew N, Zollner G, Sattabongkot J.** 2004. Infectivity of asymptomatic *Plasmodium*-infected human populations to *Anopheles dirus* mosquitoes in western Thailand. J. Med. Entomol. **41:**201–208.
24. **Singh K, Gitti RK, Diouf A, Zhou H, Gowda DC, Miura K, Ostazeski SA, Fairhurst RM, Garboczi DN, Long CA.** 2010. Subdomain 3 of *Plasmodium falciparum* VAR2CSA DBL3x is identified as a minimal chondroitin sulfate A-binding region. J. Biol. Chem. **285:**24855–24862.
25. **Srinivasan P, Beatty WL, Diouf A, Herrera R, Ambroggio X, Moch JK, Tyler JS, Narum DL, Pierce SK, Boothroyd JC, Haynes JD, Miller LH.** 2011. Binding of *Plasmodium* merozoite proteins RON2 and AMA1 triggers commitment to invasion. Proc. Natl. Acad. Sci. U. S. A. **108:**13275–13280.
26. **Riglar DT, Richard D, Wilson DW, Boyle MJ, Dekiwadia C, Turnbull L, Angrisano F, Marapana DS, Rogers KL, Whitchurch CB, Beeson JG, Cowman AF, Ralph SA, Baum J.** 2011. Super-resolution dissection of coordinated events during malaria parasite invasion of the human erythrocyte. Cell Host Microbe **9:**9–20.
27. **Chen L, Lopaticki S, Riglar DT, Dekiwadia C, Uboldi AD, Tham WH, O'Neill MT, Richard D, Baum J, Ralph SA, Cowman AF.** 2011. An EGF-like protein forms a complex with PfRh5 and is required for invasion of human erythrocytes by *Plasmodium falciparum*. PLoS Pathog. **7:**e1002199. doi:10.1371/journal.ppat.1002199.
28. **Crompton PD, Miura K, Traore B, Kayentao K, Ongoiba A, Weiss G, Doumbo S, Doumtabe D, Kone Y, Huang CY, Doumbo OK, Miller LH, Long CA, Pierce SK.** 2010. In vitro growth-inhibitory activity and malaria risk in a cohort study in Mali. Infect. Immun. **78:**737–745.
29. **Doolan DL, Mu Y, Unal B, Sundaresh S, Hirst S, Valdez C, Randall A, Molina D, Liang X, Freilich DA, Oloo JA, Blair PL, Aguiar JC, Baldi P, Davies DH, Felgner PL.** 2008. Profiling humoral immune responses to *P. falciparum* infection with protein microarrays. Proteomics **8:**4680–4694.